



Scholars Research Library

Der Pharma Chemica, 2015, 7(4):22-33
(<http://derpharmachemica.com/archive.html>)



ISSN 0975-413X
CODEN (USA): PCHHAX

Tenormin drug as save corrosion inhibitor for 304 stainless steel in hydrochloric acid solutions

A. S. Fouda^{*1}, S. M. Rashwan², M. M. Kamel² and Alaa Ibrahim¹

¹Department of Chemistry, Faculty of Science, Mansoura University, Mansoura, Egypt

²Department of Chemistry, Faculty of Science, Suez Canal University, Ismailia, Egypt

ABSTRACT

Tenormin was investigated as corrosion inhibitor for 304 stainless steel (SS) in hydrochloric acid solutions by potentiodynamic polarization, electrochemical impedance spectroscopy (EIS) and electrochemical frequency modulation (EFM) techniques. The results showed the variation in inhibition performance of the inhibitors with varying concentrations and temperatures. The maximum efficiency was found to be 92.23 % at 300 ppm concentration of Tenormin drug for the immersion period of 3 hours. Langmuir was tested to describe the adsorption behavior of Tenormin on 304 SS surface. Potentiodynamic polarization study clearly revealed that Tenormin acts as mixed type inhibitor. The results of the electrochemical impedance study showed a decrease in double layer capacitance and increase in charge transfer resistance. The results of various electrochemical techniques show good agreements with each other.

Keywords: Corrosion inhibition, stainless steel, potentiodynamic polarization, EIS, EFM

INTRODUCTION

Corrosion problems in the oil and petrochemical industry usually have been solved by the selection of suitable materials and/or by changing the environment to make it less aggressive¹. Acid solutions are widely used in the industry. The most important areas of application are acid pickling, industrial acid cleaning, acid descaling and oil well acidizing². Corrosion inhibitors are needed to reduce the corrosion rates of metallic materials in this acidmedia³⁻⁸. An inhibitor is usually added in small amount in order to slow down the rate of corrosion through the mechanism of adsorption⁹⁻¹⁰. Over the years, several inhibitors have been synthesized or chosen from existing compounds and it has been found that the best inhibitors are those that have centre for π electron donation (usually enhanced by the presence of hetero atoms in aromatic compound) while others may be gotten from extracts of naturally occurring compounds¹¹⁻¹³. A large number of organic compounds are known to be applicable as corrosion inhibitors for mild steel^{14,15}. However, only a few non-toxic and eco-friendly compounds have been investigated as corrosion inhibitors. Tryptamine, Succinic acid, L-ascorbic acid, Sulfamethoxazole and Cefatrexyl, were found to be effective inhibitors for acid environments. Dithiobiurets exhibited the best performance towards the corrosion of mild steel in HCl solutions showed very less toxicity¹⁶⁻²¹. The inhibitive effect of four antibacterial drugs, namely Ampicillin, Cloxacillin, Flucloxacillin and Amoxicillin towards the corrosion of aluminum was investigated²². The inhibition action of these drugs was attributed to blocking the surface *via* formation of insoluble complexes on the metal surface.

MATERIALS AND METHODS

2.1. Materials and solutions

Experiments were performed using 304SS samples with the following composition (weight %): C 0.08%, Mn 2.0%, Si 0.075%, Ni 8%, Cr 18%, S 0.03%, S 0.03% and balance Fe. The aggressive solution used was prepared by dilution of analytical reagent hydrochloric acid with bidistilled water. The stock solutions (6 M) of HCl 37% was prepared by dilution with bidistilled water and its concentration was checked by standard solution of Na_2CO_3 . One gram of Tenormin was dissolved in one litre of bidistilled water to give 1000 ppm and the desired concentration was obtained by dilution with bidistilled water. The concentration range of Tenormin was (50 - 300 ppm).

2.3. Electrochemical measurements

Seven test pieces of 304 SS were cut into 2 x 2 x 0.2 cm. They were abraded with emery papers (a coarse paper was used initially and then progressively finer grades were employed), degreased in acetone, rinsed with bidistilled water and finally dried between two filter papers and weighed. The test pieces were suspended by suitable glass hooks at the edge of the basin, and under the surface of the test solution by about 1 cm. Weight loss measurements were performed for 3 hours at the temperature range from 30 – 45 °C by immersing 304 SS pieces into 100 ml acid solution with and without various concentrations of Tenormin. After the specified periods of time, the specimen were taken out of the test solution, rinsed with bidistilled water, dried as before and weighed again accurately. The average weight loss at a certain time for each set of the seven samples was taken. The weight loss was recorded to nearest 0.0001 g.

2.4. Electrochemical measurements

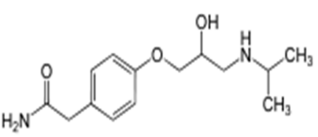
Electrochemical experiments were performed using a typical three-compartment glass cell consisted of the 304 SS specimen as working electrode (1 cm^2), saturated calomel electrode (SCE) as a reference electrode and a platinum foil (1 cm^2) as a counter electrode. The reference electrode was connected to a Luggin capillary and the tip of the Luggin capillary is made very close to the surface of the working electrode to minimize IR drop. All the measurements were done in solutions open to atmosphere under unstirred conditions. All potential values were reported versus SCE. Prior to every experiment, the electrode was abraded with successive different grades of emery paper, degreased with acetone and washed with bidistilled water and finally dried. Tafel polarization curves were obtained by changing the electrode potential automatically from (-1.0 to 0.1 V vs. SCE) at open circuit potential with a scan rate of 1 mVs^{-1} . The corrosion current is performed by extrapolation of anodic and cathodic Tafel lines to a point which gives $\log i_{\text{corr}}$ and the corresponding corrosion potential (E_{corr}) for inhibitor free acid and for each concentration of inhibitor.

Impedance measurements were carried out in frequency range from 100 kHz to 0.1 Hz with amplitude of 5 mV peak to peak using AC signals at open circuit potential. The experimental impedance was analyzed and interpreted based on the equivalent circuit. The main parameters deduced from the analysis of Nyquist diagram are the charge transfer resistance R_{ct} (diameter of high-frequency loop) and the double layer capacity C_{dl} .

Electrochemical frequency modulation, EFM, was carried out using two frequencies 2 and 5 Hz. The base frequency was 0.1 Hz, so the waveform repeats after 1 s. The higher frequency must be at least two times the lower one. The higher frequency must also be sufficiently slow that the charging of the double layer does not contribute to the current response. Often, 10 Hz is a reasonable limit. The Intermodulation spectra contain current responses assigned for harmonical and intermodulation current peaks. The larger peaks were used to calculate the corrosion current density (i_{corr}), the Tafel slopes (β_c and β_a) and the causality factors CF-2 & CF-3.

All electrochemical measurements were performed using Gamry Instrument (PCI 300/4) Potentiostat / Galvanostat/ZRA. This includes a Gamry framework system based on the ESA 400. Gamry applications include DC105 software for potentiodynamic polarization measurements, EIS300 software for electrochemical impedance spectroscopy and EFM 140 software for electrochemical frequency modulation measurements along with a computer for collecting data. Echem Analyst 6.03 software was used for plotting, graphing, and fitting data. To test the reliability and reproducibility of the measurements, duplicate experiments were performed in each case at the same conditions.

Table -1 Chemical structure, name, molecular weight and molecular formula of Tenormin drug

Inhibitor	Structure	Name	Mol. weight	Chemical formula
Tenormin		(RS)-2-(4-[2-(3-(propan-2-ylamino)propoxy)phenyl]acetamide)	325.44	C ₁₈ H ₃₁ NO ₄

RESULTS AND DISCUSSION

3.1. Weight loss method

Figure-1 shows plots for the variation of weight loss with time for the corrosion of SS in 2 M HCl containing various concentrations of Tenormin at 30°C. From the plots, it is evident that the weight loss of SS was also found to decrease with increase in the concentration of Tenormin. The weight loss of SS in the blank solution was also found to be higher than those obtained for solutions of HCl containing various concentrations of Tenormin. This indicates that Tenormin is an inhibitor for the corrosion of SS in solutions of HCl. The data of Table-2 represent the values of corrosion rates of SS and inhibition efficiency of Tenormin in HCl solution. The degree of surface coverage (θ) and inhibition efficiency (% IE) were calculated using Eq.(1):

$$\% \text{ IE} = \theta \times 100 = [1 - (\text{CR}_{\text{inh}} / \text{CR}_{\text{free}})] \times 100 \quad (1)$$

where CR_{inh} and CR_{free} are the corrosion rates in the presence and absence of inhibitor, respectively. It can be seen that the maximum of 92.2 % inhibition efficiency is achieved at 300 ppm of inhibitor concentration and %IE increases with increasing the Tenormin concentration²³. This is mainly due to the co-ordination between the metal and the hetero atom present in Tenormin.

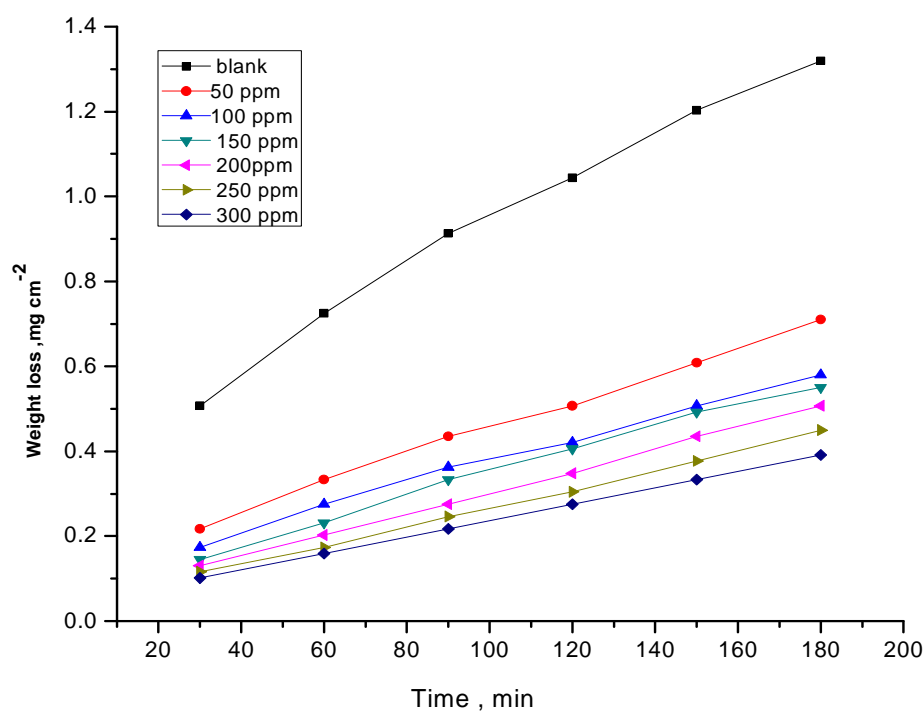


Figure-1 Weight loss-time curves for the corrosion of 304 SS in 2 M HCl in the absence and presence of different concentrations of Tenormin at 30 °C

Table-2 Corrosion Rate (CR) and inhibition efficiency (%IE) at different concentrations of inhibitor for the corrosion of 304 SS after 120 min immersion in 2 M HCl at 30°C

Conc. ppm	Tenormin	
	CR $\times 10^3$ mg cm ⁻² min ⁻¹	%IE
50	2.30	49.0
100	1.80	77.1
150	1.20	84.2
200	0.97	87.5
250	0.80	90.4
300	0.60	92.2

3.2. Effect of temperature on inhibition efficiency

The inhibition efficiency (% IE) for 304SS corrosion in the presence of various concentrations of the investigated Tenormin and at different temperatures was calculated and is listed in Table-3. The results of Table-3 shows the variation of corrosion rate (C.R.) and %IE with Tenormin concentration at different temperatures. The obtained data revealed that, the inhibition efficiency decreased with an increase in Tenormin concentration. This suggests that Tenormin species are adsorbed on the 304 SS / solution interface where the adsorbed species mechanically form a protected film on the metal surface which inhibits the action of the corrosion. A close comparison between Tables 2 and 3 revealed that weight loss of SS increases with increasing temperature indicating that the rate of corrosion of SS increases with increase in temperature. The value of inhibition efficiency was decreased with rise in temperature suggesting that physical adsorption mechanism²⁴. These results indicate that the adsorption of investigated compounds shield the metal surface at room temperature²⁵. However it may be desorbed from the surface with rise in temperature. It is also clear that corrosion rate of 304SS in the absence and presence of Tenormin obeys Arrhenius type equation as it increases with raising solution temperature. The dependence of corrosion rate (k_{corr}) on the temperature can be expressed by Arrhenius equation 2:

$$i_{\text{corr}} = A \exp(-E_a^*/RT) \quad (2)$$

where A is the pre-exponential factor and E_a^* is the apparent activation energy of the corrosion process. Arrhenius plot obtained for the corrosion of SS in 2 M hydrochloric acid solutions in the presence of different concentrations of Tenormin is shown in Figure-2. E_a^* values determined from the slopes of these linear plots are shown in Table-4. The linear regression (R^2) is close to 1 which indicates that the corrosion of 304 SS in 2 M hydrochloric acid solutions can be elucidated using the kinetic model. Table- 4 showed that the values of E_a^* for inhibited solution is higher than that for uninhibited solution, suggesting that dissolution of 304 SS is slow in the presence of Tenormin. It is known from Eq. 2 that the higher E_a^* values lead to the lower corrosion rate. This is due to the formation of a film on the SS surface serving as an energy barrier for the stainless steel corrosion²⁶. Enthalpy and entropy of activation (ΔH^* , ΔS^*) of the corrosion process were calculated from the transition state theory as given from eq. 3 (Table-4):

$$k_{\text{corr}} = (RT/h) \exp(\Delta S^*/R) \exp(-\Delta H^*/RT) \quad (3)$$

where h is Planck's constant and N is Avogadro's number. A plot of $\log(k_{\text{corr}}/T)$ vs. $1/T$ for SS in 2 M HCl with different concentrations of Tenormin gives straight lines as shown in Figure-3. Values of ΔH^* are positive. This indicates that the corrosion process is an endothermic one. The entropy of activation ΔS^* is large and negative. This implies that the activated complex represents association rather than dissociation step, indicating that a decrease in disorder takes place, going from reactants to the activated complex²⁷.

Table-3 Variation of inhibition efficiencies (%IE) and corrosion rate (CR) for various concentrations of the studied Tenormin at different temperatures

Temp. °C	Conc. ppm	Tenormin	
		CR x10 ³ mg cm ⁻² min ⁻¹	%IE
35	50	3.5	66.6
	100	2.7	74.2
	150	1.8	82.8
	200	1.5	85.7
	250	1.4	87.0
	300	1.1	89.5
40	50	5.5	63.3
	100	4.5	70.0
	150	3.5	76.6
	200	2.9	80.6
	250	2.5	83.3
	300	1.8	88.0
45	50	7.9	62.2
	100	6.3	70.0
	150	4.5	78.7
	200	3.8	81.9
	250	3.1	85.2
	300	2.8	86.9

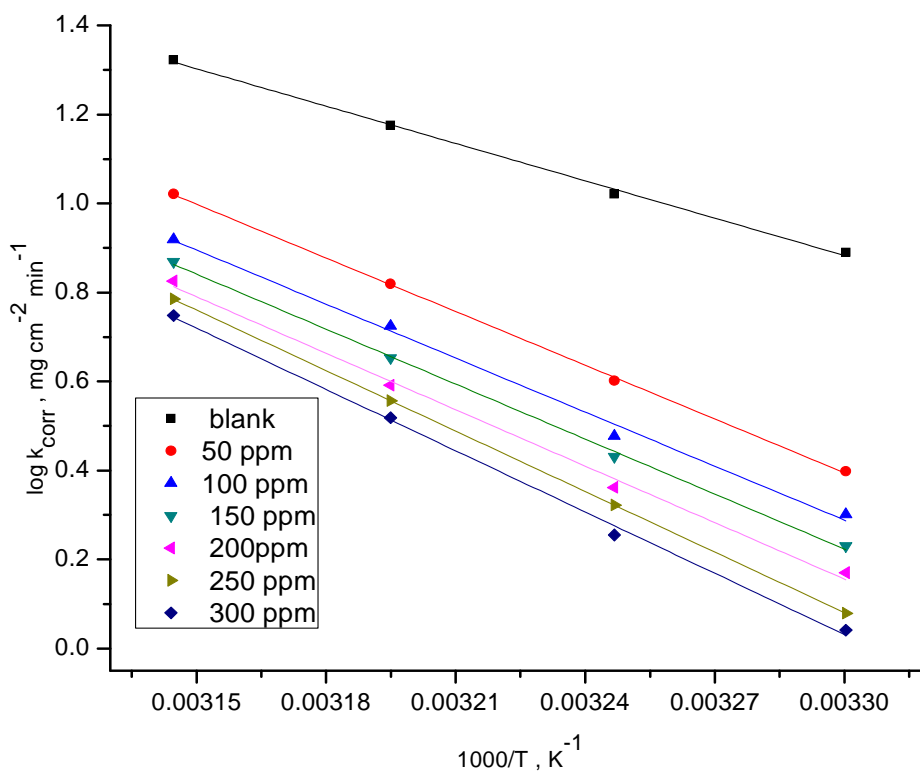


Figure-2 Arrhenius plots for 304 SS corrosion rates (k_{corr}) after 120 minute of immersion in 2 M HCl in the absence and presence of various concentrations of Tenormin

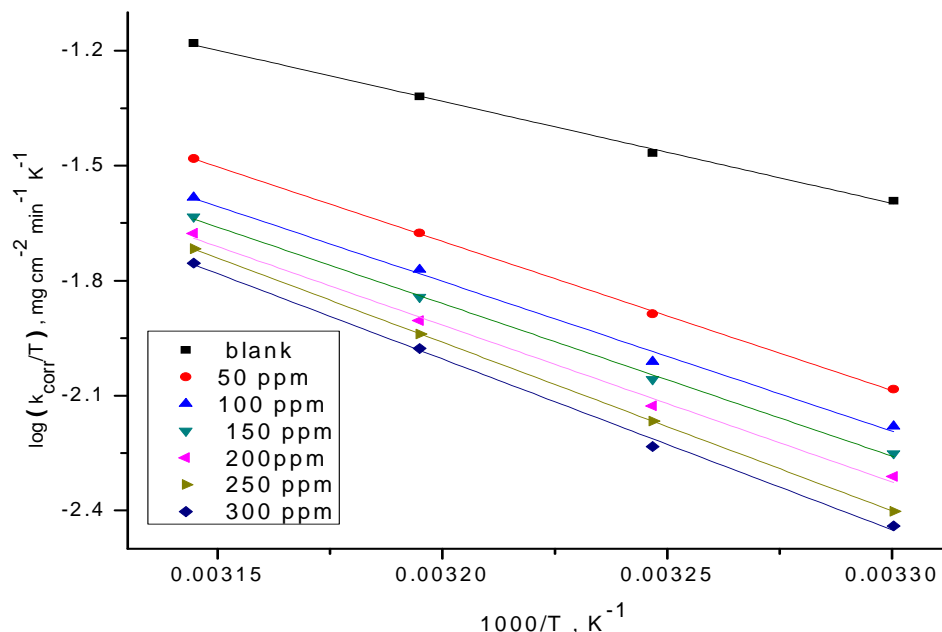


Figure-3 Transition-state for 304 SS corrosion rates (k_{corr}/T) in 2 M HCl in the absence and presence of various concentrations of Tenormin

Table-4 Activation parameters for 304 SS surface corrosion in the absence and presence of various concentrations of Tenormin in 2 M HCl

Inhibitor	Conc. ppm	Activation parameters		
		E_a kJ mol ⁻¹	ΔH^\ddagger kJ mol ⁻¹	$-\Delta S^\ddagger$ J mol ⁻¹ K ⁻¹
Blank	0.0	53.5	22.4	58.1
Tenormin	50	65.6	28.0	27.2
	100	67.6	28.8	23.3
	150	69.8	30.6	19.5
	200	74.3	31.5	15.7
	250	77.6	32.9	9.9
	300	78.3	34.0	5.9

3.3. Adsorption isotherms

Adsorption isotherm values are important to explain the mechanism of corrosion inhibition of organo-electrochemical reactions. The most frequently used isotherms are Langmuir isotherm (Figure-4). Thermodynamic parameters for the adsorption of different inhibitors on 304SS surface in 2 M HCl at different temperatures was listed in Table -5

Table -5 Thermodynamic adsorption parameters for the adsorption of Tenormin on stainless steel in 2 M HCl at different temperatures

Inhibitor	Temp. °C	$K_{\text{ads}} \times 10^{-4}$ M ⁻¹	$-\Delta G^\circ_{\text{ads}}$ kJ mol ⁻¹	$-\Delta H^\circ_{\text{ads}} \times 10^{-5}$ kJ mol ⁻¹	$-\Delta S^\circ_{\text{ads}}$ J mol ⁻¹ K ⁻¹
Tenormin	30	270	24.2	12.9	80.0
	35	237	24.3		78.9
	40	210	24.4		77.9
	45	175	24.3		76.3

From Table-5 it was found that: The negative values of $\Delta G^\circ_{\text{ads}}$ reflect that the adsorption of studied Tenormin on 304 SS in 2 M HCl solution is spontaneous process²⁸. $\Delta G^\circ_{\text{ads}}$ values increase (become less negative) with an increase of temperature which indicates the occurrence of exothermic process at which adsorption was unfavorable with increasing reaction temperature as the result of the inhibitor desorption from the stainless steel surface²⁹. It is usually accepted that the value of $\Delta G^\circ_{\text{ads}}$ around -20 kJ mol⁻¹ or lower indicates the electrostatic interaction between charged metal surface and charged organic molecules in the bulk of the solution³⁰. The negative sign of $\Delta H^\circ_{\text{ads}}$ reveals that the adsorption of inhibitor molecules is an exothermic process. Generally, an exothermic adsorption process suggests either physisorption or chemisorption while endothermic process is attributed to chemisorptions^{31,32}. Generally, enthalpy values up to 41.9 kJ mol⁻¹ are related to the electrostatic interactions between charged molecules and charged metal (physisorption) while those around 100

kJmol^{-1} or higher are attributed to chemisorption. In the case of investigated compounds, the absolute values of enthalpy are relatively low, approaching those typical of physisorption. The values of $\Delta S_{\text{ads}}^{\circ}$ in the presence of investigated compounds are large and negative that is accompanied with exothermic adsorption process³³. The experimental data give good curves fitting for the applied adsorption isotherm as the correlation coefficients (R^2) were in the range 0.938-0.999. K_{ads} value decreases with the increase of temperature from 30 to 45 °C.

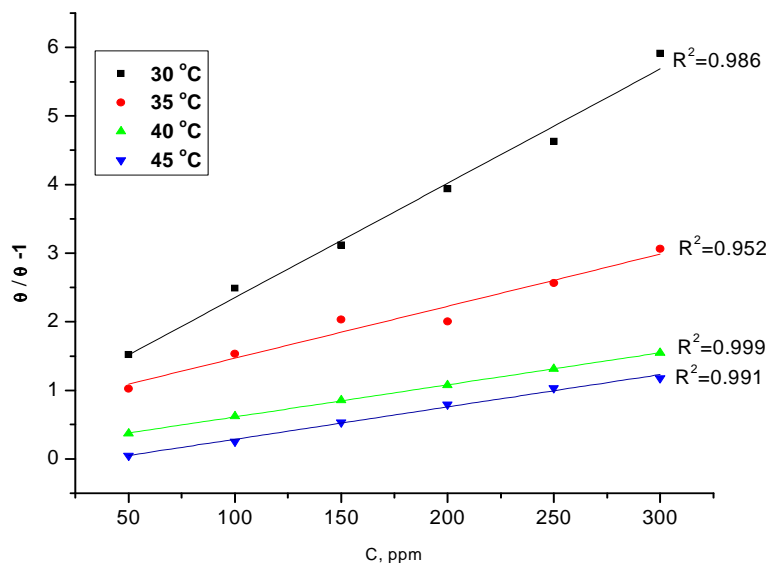


Figure-4 Langmuir isotherm of Tenormin on 304 SS surface in 2 M HCl at different temperatures

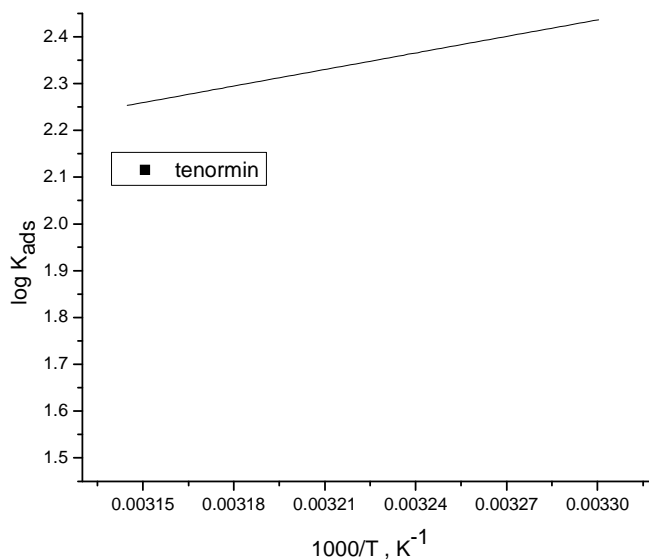


Figure-5 ($\log k_{\text{ads}}$) vs ($1/T$) for the corrosion of 304 SS in 2 M HCl in the presence of Tenormin

3.4. Potentiodynamic Polarization Measurements

Polarization measurements were carried out in order to gain knowledge concerning the kinetics of the cathodic and anodic reactions. Figure-5 presents the results of the effect of Tenormin on the cathodic and anodic polarization curves of 304 SS in 2 M HCl. Similar curves for other compounds were obtained but not shown. It could be observed that both the cathodic and anodic reactions were suppressed with the addition of investigated compounds, which suggested that these compounds reduced anodic dissolution and also retarded the hydrogen evolution reaction. Electrochemical corrosion kinetics parameters, i.e. corrosion potential (E_{corr}), cathodic and anodic Tafel slopes (β_a , β_c) and corrosion current density (i_{corr}) obtained from the extrapolation of the polarization curves, were given in Table-6. The parallel cathodic Tafel curves in Figure-5 suggested that the hydrogen evolution is activation-controlled and the reduction mechanism is not affected by the presence of the inhibitor. The region between linear part of cathodic and anodic branch of polarization curves becomes wider as the

inhibitor is added to the acid solution. Similar results were found in the literature³⁴. The values of β_a and β_c changed slightly with increasing inhibitor concentration indicated the influence of these compounds on the kinetics of metal dissolution and of hydrogen evolution. Due to the presence of some active sites, such as aromatic rings, hetero-atoms in the studied compound for making adsorption, they may act as adsorption inhibitors. Being adsorbed on the metal surface, these compounds controlled the anodic and cathodic reactions during corrosion process, and then their corrosion inhibition efficiencies are directly proportional to the amount of adsorbed inhibitor. The functional groups and structure of the inhibitor play important roles during the adsorption process. On the other hand, an electron transfer takes place during adsorption of the neutral organic compounds at metal surface³⁵. As it can be seen from Table-6, the studied inhibitor reduced both anodic and cathodic currents with a slight shift in corrosion potential (47 mV). According to Ferreira and others³⁶, if the displacement in corrosion potential is more than 85mV with respect to corrosion potential of the blank solution, the inhibitor can be seen as a cathodic or anodic type. In the present study, the displacement was 47 mV which indicated that the studied inhibitor is mixed-type inhibitor. The results obtained from Tafel polarization showed good agreement with the results obtained from weight loss method. The surface coverage (θ) and % IE were calculated using Eq.4:

$$\%IE = \theta \times 100 = [1 - (i_{\text{corr}}/i_{\text{corr}}^{\circ})] \times 100 \quad (4)$$

Where i_{corr} and i_{corr}° are the current densities in presence and absence of inhibitor, respectively.

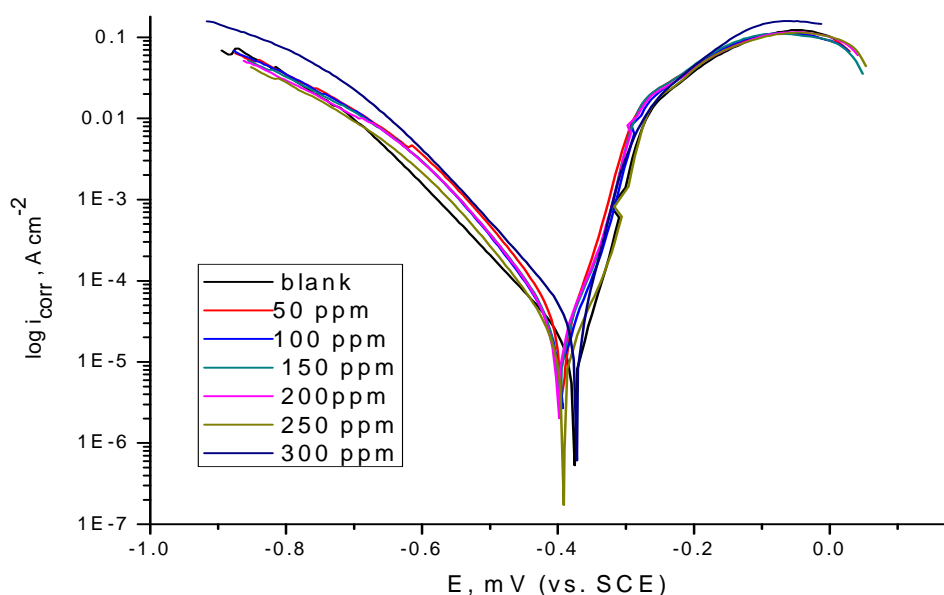


Figure – 6 Potentiodynamic polarization curves for the dissolution of 304SS in 2 M HCl in the absence and presence of different concentrations of Tenormin at 30°C

Table-6 Effect of concentrations of various compounds on the free corrosion potential (E_{corr}), corrosion current density (i_{corr}), Tafel slopes (β_c , β_a), corrosion rate (k_{corr}), degree of surface coverage (θ), and inhibition efficiency (%IE) of 304 SS in 2 M of HCl at 30°C

Inh	[Inh.] ppm	$-E_{\text{corr}}$ mV vs SCE	i_{corr} mA cm ⁻²	β_c mV dec ⁻¹	β_a mV dec ⁻¹	k_{corr} mmy ⁻¹	θ	%IE
blank	0.0	372	598	135	64	27.33	----	----
Tenormin	50	393	285	89	46	13.01	0.523	52.3
	100	399	260	85	60	11.95	0.562	56.2
	150	375	232	100	51	10.62	0.612	61.2
	200	395	190	85	51	8.67	0.682	68.2
	250	391	174	92	65	7.94	0.709	70.9
	300	375	149	110	39	6.79	0.751	75.1

3.5. Electrochemical Impedance Spectroscopy Measurements

Nyquist plots of 304 SS in uninhibited and inhibited acid solutions containing different concentrations of Tenormin are presented in Figure-7. EIS spectra obtained consists of one depressed capacitive loop. The increased diameter of capacitive loop obtained in 2 M HCl in presence of Tenormin indicated the inhibition of corrosion of 304SS. The high frequency capacitive loop may be attributed to the charge transfer reaction. Corrosion kinetic parameters derived from EIS measurements and inhibition efficiencies are given in Table-7. Double layer capacitance (C_{dl}) and

charge transfer resistance (R_{ct}) were obtained from EIS measurements as described elsewhere³⁷. It is apparent from Table-7 that the impedance of the inhibited system amplified with the inhibitor the C_{dl} values decreased with inhibitor. This decrease in C_{dl} results from a decrease in local dielectric constant and/or an increase in the thickness of the double layer, suggested that inhibitor molecules inhibit the iron corrosion by adsorption at the metal/acid interface³⁸. The depression in Nyquist semicircles is a feature for solid electrodes and often referred to as frequency dispersion and attributed to the roughness and other inhomogeneities of the solid electrode³⁹. In this behavior of solid electrodes, the parallel network: charge transfer resistance-double layer capacitance is established where an inhibitor is present. For the description of a frequency independent phase shift between an applied ac potential and its current response, a constant phase element (CPE) is used which is defined in impedance representation as in Eq. (5)

$$Z_{CPE} = Y_0^{-1}(i\omega)^{-n} \quad (5)$$

where, Y_0 is the CPE constant, ω is the angular frequency (in rad s^{-1}), $i^2 = -1$ is the imaginary number and n is a CPE exponent which can be used as a gauge of the heterogeneity or roughness of the surface⁴⁰. Depending on the value of n , CPE can represent resistance ($n = 0$, $Y_0 = R$), capacitance ($n = 1$, $Y_0 = C$), inductance ($n = -1$, $Y_0 = L$) or Warburg impedance ($n = 0.5$, $Y_0 = W$). Figure-7 showed the electrical equivalent circuit employed to analyze the impedance spectra. Excellent fit with this model was obtained for all experimental data. The surface coverage (θ) and % IE were calculated using Eq. 6:

$$\%IE = \theta \times 100 = [1 - (R_{ct}/R_{ct}^{\circ})] \times 100 \quad (6)$$

where R_{ct} and R_{ct}° are the charge transfer resistances in absence and presence of inhibitor, respectively.

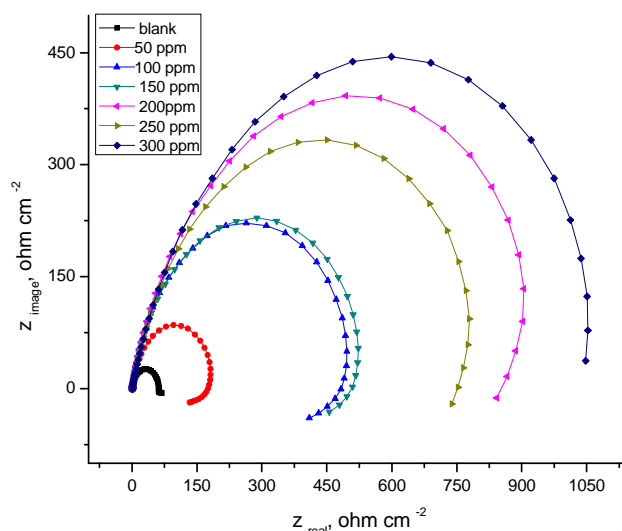


Figure-7 Nyquist plots for the corrosion of 304SS in 2 M HCl in the absence and presence of different concentrations of Tenorminat at 30°C

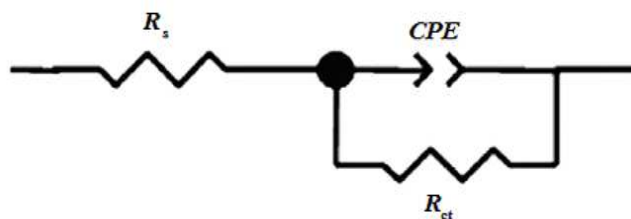


Figure-8 Electrochemical equivalent circuit used to fit the impedance measurements that include a solution resistance (R_s), a constant phase element (CPE) and a polarization resistance or charge transfer (R_{ct})

3.6. Electrochemical Frequency Modulation Measurements

EFM is a nondestructive corrosion measurement like EIS; it is a small signal Ac technique. Unlike EIS, however, two sine waves (at different frequencies) are applied to the cell simultaneously. The great strength of the EFM is the causality factors which serve as an internal check on the validity of the EFM measurement⁴¹. With the causality factors the experimental EFM data can be verified. The results of EFM experiments are a

spectrum of current response as a function of frequency. The spectrum is called the intermodulation spectrum. The spectra contain current responses assigned for harmonical and intermodulation current peaks. The larger peaks were used to calculate the corrosion current. The inhibition efficiencies, % IE calculated from Equation 3 increase with increasing the studied inhibitor concentrations. The two frequencies may not be chosen at random. They must both be small, integer multiples of a base frequency that determines the length of the experiment. Intermodulation spectra obtained from EFM measurements were constructed for iron 2 M HCl solutions as a function of 300 ppm of Tenormin at 30°C. Each spectrum is a current response as a function of frequency; data not shown here. Corrosion kinetic parameters, namely corrosion current density (i_{corr} , Tafel constants (β_a, β_c) and causality factors (CF-2, CF-3) were listed Table-8 as a function of concentrations of investigated compounds at 30°C. The causality factors in Table-8, which are very close to theoretical values according to the EFM theory, should guarantee the validity of Tafel slopes and corrosion current densities. The standard values for CF-2 and CF-3 are 2.0 and 3.0, respectively⁴².

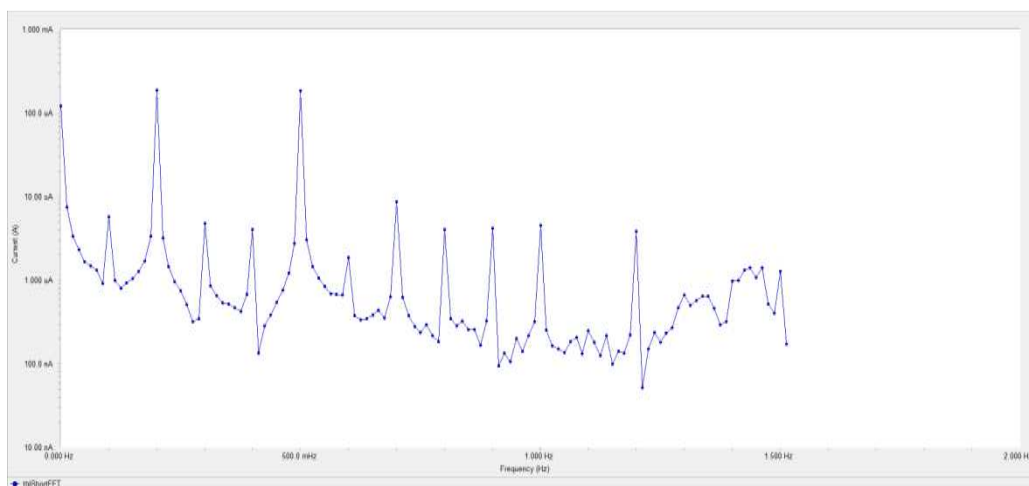


Figure-8EFM spectra for SS in 2M HCl in the presence of 50 ppm Tenormin

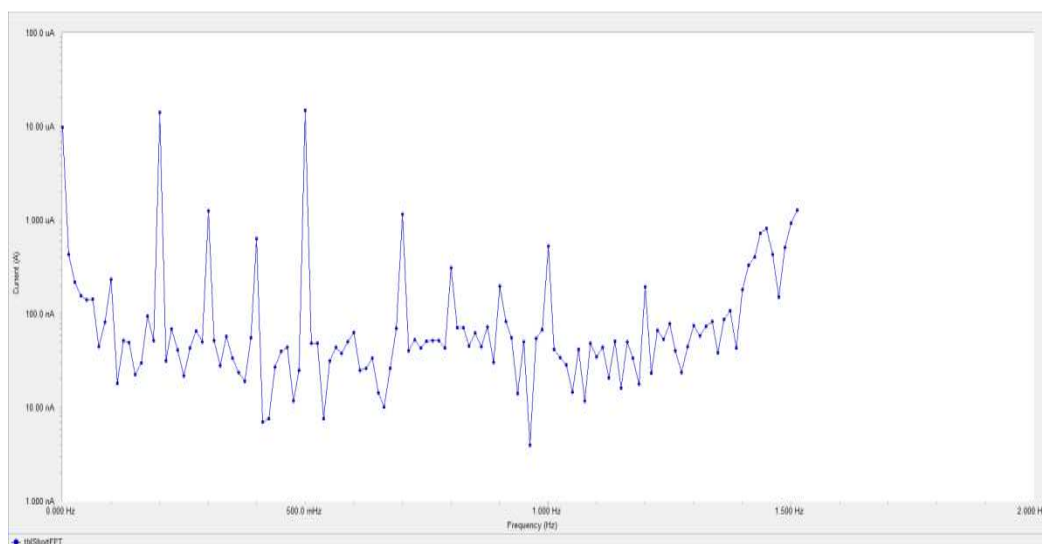


Figure-9EFM spectra for SS in 2M HCl in the presence of 300 ppm Tenormin

Table-7EIS parameters for the corrosion of SS in 2 M HCl in the absence and presence of different concentrations of investigated compound at 30°C

Inhibitor	Conc. ppm	$C_{dl} \times 10^{-5}$ $\mu F cm^{-2}$	R_{ct} Ωcm^2	θ	% IE
Blank	0.0	22.99	62.4	---	---
Tenormin	50	8.16	191.3	0.674	67.4
	100	7.15	488.7	0.872	87.2
	150	8.22	527.8	0.882	88.2
	200	10.37	816.9	0.924	92.4
	250	9.751	952.8	0.935	93.5
	300	12.97	1147.0	0.946	94.6

Table-8 Electrochemical kinetic parameters obtained from EFM technique for SS in 2 M HCl in the absence and presence of different concentrations of Tenormin

Inhibitor	Conc. ppm	i_{corr} , $\mu A cm^{-2}$	β_a , $m V dec^{-1}$	β_c , $m V dec^{-1}$	CF-2	CF-3	CR mpy	% IE
Blank	0.0	216.8	70	82	1.6	2.8	99.05	
Tenormin	50	127.1	69	94	1.8	2.8	58.09	41.4
	100	44.71	72	98	1.7	3.1	20.43	79.4
	150	44.07	77	100	1.9	2.7	20.14	79.7
	200	29.95	78	120	1.9	3.2	13.69	86.2
	250	26.18	77	123	2.0	2.9	11.96	87.9
	300	22.17	79	132	2.1	3.5	10.13	89.8

The results obtained from weight loss, potentiodynamic polarization, electrochemical frequency modulation and impedance techniques are in a good agreement but it is of interest to note that, the values of % IE given by electrochemical techniques are higher than those obtained by weight loss measurements; this may be due to the fact that the electrochemical measurements were carried out on freshly prepared solutions.

3.7. Mechanism of Inhibition

The inhibitive action of organic compounds depends of their structure and functional groups, nature of the metal and aggressive medium [27, 28]. The inhibitory action of Tenormin drug may be due to one of the following mechanisms: (i) physical adsorption of the molecules on the metal surface; (ii) electrostatic interactions between protonated nitrogen atoms and already adsorbed Cl atoms; (iii) coordination due to donor-acceptor interactions between the unshared electron pairs of nitrogen and oxygen atoms (iv) the π -electrons from the aromatic rings may also interact with the vacant d-orbitals of the atoms of the metal at the interface; (v) since the high molecular weight of Tenormin the inhibition may be effected by hindering of attacks by Cl⁻ ions due to wider surface covered by large molecules of Tenormin.

REFERENCES

- [1] Heydari M., Ravari F. B., Dadgarineghad A., GU. *J. Sci.* 24(3) (2011) 507.
- [2] Rozenfeld, I. L., "Corrosion Inhibitors", McGraw-Hill, New York, (1981).
- [3] Benali O., Larabi L., Traisnel M., Gengembre L., Harek Y., *Appl. Surf. Sci.* 253 (2007) 6130.
- [4] Merah S., Larabi L., Benali O., Harek Y., *Pigm. Resin. Technol.* 37 (5) (2008) 291.
- [5] Benali O., Larabi L., Harek Y., *J. Appl. Electrochem.* 39 (2009) 769.
- [6] Benali O., Larabi L., Harek Y., *J. Saud. Chem. Soc.* 14 (2) (2010) 231.
- [7] Benali O., Larabi L., Tabti B., Harek Y., *Anti-Corros. Meth. Mat.* 52 (2005) 280.
- [8] Benali O., Larabi L., Mekelleche S.M., Harek Y., *J. Mater. Sci.* 41 (2006) 7064.
- [9] Eddy N. O., *International J. Phys. Sci.* 4 (4) (2009) 165.
- [10] Bouyanzer A., Hammouti B., *Pigment and Resin Tech.* 33(5) (2004) 287.
- [11] Eddy N. O., Ekwumemgbo P., Odoemelam S. A., *Int. J. Phys. Sci.* 3(11) (2008) 275.
- [12] Eddy N. O., Odoemelam S. A., Akpanudoh N. W., *Res. J. Pure Appl. Sci.* 4(12) (2008) 1963.
- [13] Eddy N. O., Odoemelam S. A., Mbaba A. J., *Afri. J. Pure Appl. Chem.* 2(12) (2008) 132.
- [14] Ahamad, I.; Quraishi, M.A. *Corrosion Sci.*, 2010, 52(2), 651-656.
- [15] Quraishi, M. A.; Shukla, Sudhish Kumar. *Mater. Chem. Phys.*, 2009, 113(2), 685-689.
- [16] Moretti, G.; Guidi, F.; Grion, G. *Corrosion Sci.*, 2004, 46(2), 387-403.
- [17] Giacomelli, F. C.; Giacomelli, C.; Amadori, M. F.; Schmidt, V.; Spinelli, A. *Mater. Chem. Phys.*, 2004, 83(1), 124-128.
- [18] Ferreira, E. S.; Giacomelli, C.; Giacomelli, F. C.; Spinelli, A. *Mater. Chem. Phys.*, 2004, 83(1), 129-134.
- [19] El Sherbini, E. E. F. *Mater. Chem. Phys.*, 1999, 60(3), 286-290.
- [20] Morad, M. S. *Corrosion Sci.*, 2008, 50(2), 436-448.

- [21] Quraishi, M. A.; Rawat, J.; Ajamal, M. *J. Appl. Electrochem.*, **2000**, 30(6), 745- 751.
- [22] Abdallah, M. *Corrosion Sci.*, **2004**, 46(8), 1981- 1996.
- [23] Zaaferany A. and Abdallah M., *Electrochem. Sci.*, **5 (2010)** 18-28
- [24] Ameh PO, Eddy NO (**2013**). *Res. Chem. Intermediates*.pp.1- 9.
- [25] Petchiammal A, Deepa RP, Selvaraj S, KalirajanK (**2012**). *Res. J. Chem. Sci.* 2(4):24-34
- [26] Fouda A. S., Al-Sarawy A. A., El-Katori E.E, *Desalination* 201 (**2006**) 1-13
- [27] Gece G., *Corros. Sci.* 50 (**2008**) 2981-2992
- [28] Tang L., Lie X., Si Y., Mu G. and Liu G., *Mater. Chem. Phys.* 95 (**2006**) 29
- [29] Tang L., Murad G. and Liu G., *Corros. Sci.* 45 (**2003**) 2251
- [30] Putilova I. N., Balzin S. A. and Barannik V. P., *Metallic Corrosion Inhibitors*, Pergamon Press, (**1960**) 31
- [31] Khamis E., *Corrosion (NACE)* 46 (**1990**) 476
- [32] Li X. and Tang L., *Mater. Chem. Phys.* 90 (**2005**) 286
- [33] El-Awady A. A., Abd El-Nabey B. and Aziz S. G., *Electrochem. Soc.* 139 (**1992**) 2149
- [34] Abd El-Rehim S. S., Hassan H. H. and Amin M. A., *Mater. Chem. Phys.* 70 (**2001**) 64
- [35] Singh A. K., Quraishi M. A., *Corros. Sci.* 52 (**2010**) 1373-1385
- [36] Bentiss F., Jama C., Mernari B., Attari H. E., Kadi L. E., Lebrini M., Traisnel M., Lagrenee M., *Corros. Sci.* 51(**2009**)1628-1635
- [37] Ashassi-Sorkhabi H., Seifzadeh D., Hosseini M. G., *Corros. Sci.* 50 (**2008**) 3363-3370 *Int. J. Electrochem. Sci.*, Vol. 9, 2014 364
- [38] Popova A., Christov M., *Corros. Sci.* 48 (**2006**) 3208-3221
- [39] Gamry *Echem Analyst Manual*, **2003**
- [40] Bosch R.W., Hubrecht J., Bogaerts W.F., Syrett B.C.,: *Monitoring Corrosion* 57, 60 ,(2001)
- [41] Abdel-Rehim S.S., Khalid K.F., Abd-Elshafi N.S., *Electrochem. Acta* 51,3269-3277, (2006)
- [42] 42.Singh A. K., Quraishi M. A., *J. Mater. Environ. Sci* (**2010**) 101-110
- [43] S. Chitra, K. Parameswari, C. Sivakami, and A. Selvaraj, *Chemical Engineering Research Bulletin*, vol. 14, pp. 1-6, **2010**.
- [44] R. V. Saliyan and A. V. Adhikari, *Indian Journal of Chemical Technology*, vol. 16, no. 2, pp. 162-174, **2009**.
View at Scopus